centrifuged to remove undigested debris, and the DNA-containing supernatant fraction was incubated at 95°C for 8 min.

33. Nylon filters (Pall Biodyne-B, 0.45 μm) were briefly rinsed in water and mounted on a Bio-Rad dot-blot apparatus. A sample (4 μl) of each final amplification product was denatured in 0.4 M NaOH and 25 mM EDTA for 5 min and spotted on the filter. The DNA was cross-linked to the filter with a Stratalinker (Stratagene) set at auto cross-link. The filters were prehybridized in 5× SSPE and 0.5% SDS at 50°C for 30 min; a ^{32}P end-labeled oligonucleotide (1 ng) was added to this prehybridization solution, and the whole reaction was incubated at 50°C for 45 to 60 min. The hybridized filters were washed briefly in 2× SSPE and 0.1% SDS at room temperature, and then incubated for 10 min in 3 M tetramethyl ammonium chloride, 0.2% SDS, and 50 mM tris (pH 8.0), at the following temperatures: for α_s codon 201, 64.5°C; α_s codon 227, 67°C; α_{i2} codon 179, 61.5°C; α_{i2} codon 205, 67.5°C. The filters were exposed to Kodak X-AR film for 2 to 6 hours at −70°C with intensifying screens. For subsequent hybridization with different oligonucleotides the Nylon filters were stripped by boiling the filters for 5 min in 2× SSPE and 0.1% SDS and then processed as described above. Oligonucleotide probes used to screen the tumors were specific for wild type and for each missense or nonsense single-base change at the two codons; base changes that would be silent were not tested. The probe sequences (with the wild-type codon in bold type) were as follows: α_s codon 201, TTCGCTGCC**GT**GTCCTGACT (six mutant codons tested); α_s codon 227, GTGGGTGGC**CAG**CGCGATGA (eight mutant codons tested); α_{i2} codon 179, TACGGACCC**G**CGTAAAGACC (six mutant codons tested); α_{i2} codon 205, GTGGGTGGT**CAG**CGGTCTGA (eight mutant codons tested).

34. We thank S. Phipps (Cetus) for technical assistance, C. Johnson (Cetus) for histologic analysis of paraffin-embedded tissue, H. Bos (University of Leiden) for reading the manuscript, R. Brescia (UCSF) for review of ovarian tumors and reading the manuscript, R. L. Davis (UCSF) for review of pituitary adenoma pathological slides, C. B. Wilson (UCSF) for providing pituitary tumor specimens, S. Masters for providing ovarian tumor specimens, A. Spada (University of Milan) for providing biochemically characterized pituitary samples, D. Spasic, L. Goda, and C. Levenson (Cetus) for synthetic oligonucleotides, and M. Dallman, D. Gospodarowicz, and R. Jaffe (UCSF) for advice. Supported in part by NIH grants (H.R.B. and C.A.L.) and grants from the Austrian Fonds Zur Forderung Der Wissenschaftlichen Forschung (K.G. and H.F.).

12 February 1990; accepted 30 May 1990

Metalloantibodies

BRENT L. IVERSON, SHEILA A. IVERSON, VICTORIA A. ROBERTS, ELIZABETH D. GETZOFF, JOHN A. TAINER, STEPHEN J. BENKOVIC, RICHARD A. LERNER

A metalloantibody has been constructed with a coordination site for metals in the antigen binding pocket. The Zn(II) binding site from carbonic anhydrase B was used as a model. Three histidine residues have been placed in the light chain complementarity determining regions of a single chain antibody molecule. In contrast to the native protein, the mutant displayed metal-dependent fluorescence-quenching behavior. This response was interpreted as evidence for metal binding in the three-histidine site with relative affinities in the order Cu(II) > Zn(II) > Cd(II). The presence of metal cofactors in immunoglobulins should facilitate antibody catalysis of redox and hydrolytic reactions.

CATALYTIC ANTIBODIES HAVE NOW been induced with haptens that are designed to use a number of different strategies for effecting catalysis [for reviews, see (*1, 2*)]. Distortion, charge stabilization, and proximity have all been used to advantage. Antibody side chains in the binding pocket can participate directly in some of the reactions. Binding sites modified covalently and by site-directed mutagenesis have also yielded increases in catalytic rate. Finally, metal complexes have been enlisted to effect catalysis of simultaneously bound substrates for specific hydrolysis of the peptide bond.

The advent of facile systems for the recombination and expression of the antibody repertoire in bacteriophage λ allows consideration of a new approach for utilizing antibody-bound cofactors (*3–6*). In this system a cofactor binding light chain could be combined with a heavy chain library derived from the polymerase chain reaction (PCR) products of a mouse previously immunized with a substrate or substrate analog of interest. Ideally, significant binding of substrate can be maintained by the heavy chain (*3, 4*), and a few combinations will be produced in which the substrate is bound in a suitable position to facilitate reaction with the cofactor. In this approach the diversity of the antibody repertoire is used to enhance a catalytic design. Successful implementation of this strategy requires the production of antibodies that present cofactors in proximity to bound antigen. We report the production of an antibody that simultaneously binds the reporter antigen fluorescein and directly coordinates metal ions such as Cu(II).

The general design strategies for remodeling antibodies is the subject of a separate report (*7*). Briefly, for the work described here, a computer search was conducted on the known catalytic metal binding sites in metalloenzymes, and the backbone configurations around these sites were compared with those of the complementarity determining regions (CDRs) in antibody light chains. A striking similarity was discovered between the antiparallel β-sheet structure around the three His ligand residues of the zinc binding site of carbonic anhydrase B (*8*) and the β-sheet structure around residues 34, 89, and 91 [numbering of Kabat *et al.* (*9*)], in CDRs L1 and L3 of antibody light chains (Fig. 1, A and B). Substitution of these three antibody residues with His should form a binding site that resembles that of the natural metalloenzyme (Fig. 1B) (*10*). Furthermore, a bound metal will be located deep in the groove of the binding site (see Fig. 1C) with the metal protruding slightly toward the heavy chain. This should make the vacant coordination site on the metal atom highly accessible to substrate. Since the β-sheet structure in this region is rigorously conserved among the antibodies of known structure (*11, 12*), our design should be generally applicable to antibody light chains.

The single chain fluorescein binding molecule (referred to here as native sequence protein) (*13*) with the 212 linker derived from the antibody 4-4-20 was chosen for our metal binding studies for several reasons. First, the three-dimensional structure of the parent antibody combining site with bound fluorescein is known (*14*). Second, the gene has been cloned into a highly efficient expression vector (*13*), which is readily amenable to site-directed mutagenesis. Third, the six Trp residues in the molecule surround the new metal binding site, which suggests that bound metals such as Cu(II) would effectively quench Trp fluorescence (Fig. 1D). Model building indicated metal to nearest atom distances for five Trp residues of 5 to 10 Å and for one Trp residue of 15 Å. Finally, bound fluorescein was expected to be useful as a spectroscopic probe for locating bound metal in the properly folded antibody combining site (Fig. 1D).

Histidine residues were introduced into L1 at Arg^{34} and L3 at Ser^{89} and Ser^{91}. Since Ser^{91} and Arg^{34} form hydrogen bonds to the bound fluorescein (*14*), the fluorescein binding constant should be lower for the mutant protein, but should still be measurable because of the high binding constant for the native sequence protein (*13*). Inspection of

B. L. Iverson, S. A. Iverson, V. A. Roberts, E. D. Getzoff, J. A. Tainer, R. A. Lerner, Departments of Molecular Biology and Chemistry, The Research Institute of Scripps Clinic, La Jolla, CA 92037.
S. J. Benkovic, Department of Chemistry, Pennsylvania State University, University Park, PA 16802.

the crystal structure of 4-4-20 (*14*) further revealed that Tyr^{36} might interfere with the putative metal binding site, so this was changed to Leu, which in fact occupies this framework position in some antibodies.

The four mutations were introduced into the light chain of the 4-4-20 single chain molecule by two successive rounds of site-directed mutagenesis by the method of Nakamaye and Eckstein (*15*). The two mutations were introduced into CDR3 at Ser^{89} → His and Ser^{91} → His by using one 30 nucleotide (nt) segment. A subsequent round of mutagensis was performed to modify the two residues in CDR1, Arg^{34} → His and Tyr^{36} → Leu, with another 30-nt oligonucleotide. A single clone was identified and shown by DNA sequencing to contain all four mutations in the light chain region. The vector used for mutagenesis contained the 4-4-20/202′ gene (*13*), but lacked the promoter region to allow for more efficient production of single-stranded DNA and replication of the plasmid in *Escherichia coli* strain TG1 during the mutagenesis. Once the quadruple mutant (QM 202′) was identified by sequencing, the CsCl-purified plasmid was digested with the appropriate restriction enzymes to remove the light chain portion of the molecule leaving the 202′ linker behind. The modified light chain was ligated into an expression vector that contained a new linker designated 212, the native sequence heavy chain, and a λ promoter (*16*). The *Escherichia coli* strain GX6712 (*17*) was transformed with the completed mutant construct (QM 212) for expression. This *E. coli* strain contains the C1857 temperature-sensitive λ repressor gene used for heat induction of the λ promoter by raising the temperature of the culture (Fig. 2).

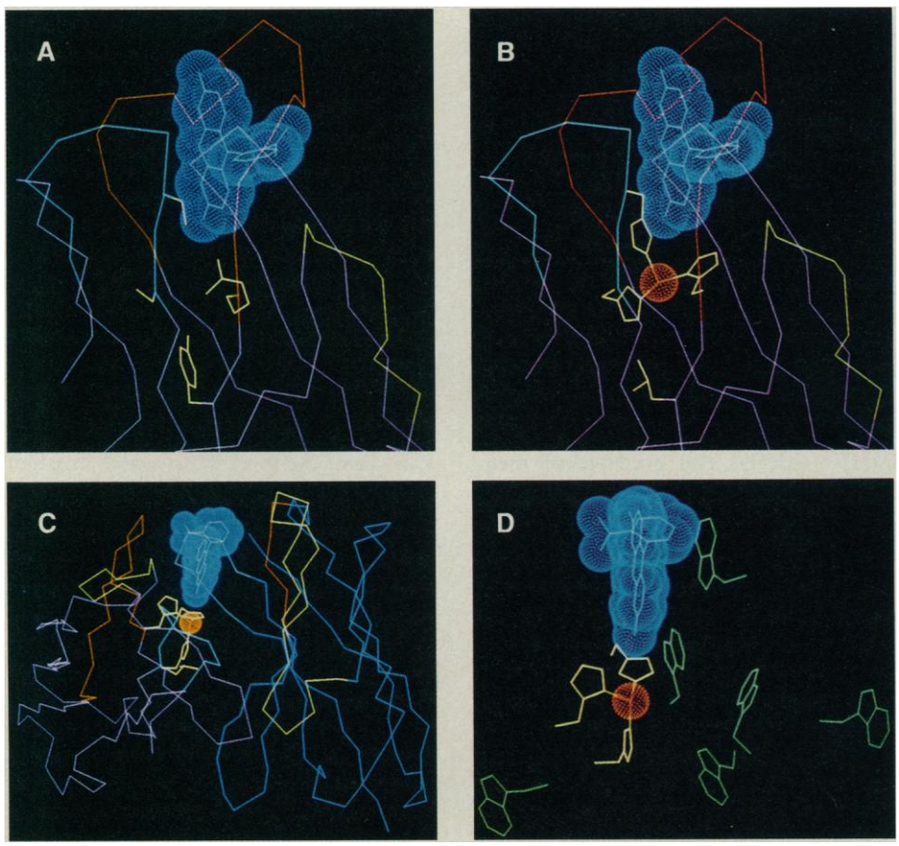

Fig. 1. (**A**) View of the 4-4-20 light chain CDRs with the bound fluorescein molecule displayed for reference. The highlighted residues are Arg^{34}, Tyr^{36}, Ser^{89}, and Ser^{91}, which were mutated to create the mutant QM 212. Note the β-pleated sheet backbone in this region as well as interaction of Arg^{34} and Ser^{91} with the fluorescein molecule. (**B**) Same view as before except the three His side chains and metal from the Zn(II) binding site in carbonic anhydrase B have been substituted into the appropriate location in the light chain CDRs. The side chain of Tyr^{36} has also been changed to Leu. (**C**) View of the α-carbon backbone for the entire Fv region of the 4-4-20 structure with bound fluorescein. The carbonic anhydrase B Zn(II) binding site has been substituted into the protein as before. The light chain backbone is shown in lavender, the heavy chain backbone is in blue, and the CDRs are in various colors. In this structure, the metal atom is deep in the antibody combining pocket with the metal protruding toward the heavy chain CDRs. Note also the close proximity of the metal atom to fluorescein. (**D**) View of the proposed metal binding site in QM 212 showing the relative locations of the bound fluorescein and the six Trp side chains in the molecule. This fortuitous proximity of metal to fluorophore was used to identify binding as well as indicate the location of bound metal in QM 212.

We anticipated that appropriately bound metal ions would efficiently quench Trp fluorescence by a static mechanism. In studies on model systems and metalloproteins, Cu(II), along with Ni(II), Mn(II), Co(II), and Cd(II), have been identified as being particularly efficient in quenching Trp fluorescence (*18–21*). Zinc(II) was not expected to directly quench Trp fluorescence (*21*, p. 259).

The QM 212 and native sequence proteins have Trp emission maxima at 343 and 352 nm, respectively. This blue shift indicates that Trp residues are on average in a more hydrophobic environment (*21*, p. 355) in the mutant protein. In the presence of 0 to 30 μM Cu(II) the Trp fluorescence of the native sequence protein displayed minimal quenching and no saturation behavior was observed (see Fig. 3A). A Stern-Volmer plot of this data was linear and gave a quenching constant of $1.2 \times 10^4\ M^{-1}$. In contrast, the Trp fluorescence of QM 212 was dramatically quenched by Cu(II) until less than 20% residual fluorescence remained. The sigmoidal shape of the QM 212 quenching curve depended on sodium phosphate concentration, which was taken to be the result of nonspecific buffer interactions with metal or protein or both. Thus one cannot extract a true binding constant from the data, but a lower estimate of $\sim 2 \times 10^5\ M^{-1}$ can be derived from the midpoint of the quenching curve. This efficient fluorescence quenching indicates the Cu(II) atom is near most of the Trp residues, which is consistent with binding occurring in the three-histidine site.

Addition of EDTA to a final concentration of 100 μM in a solution containing 150 nM QM 212 and 30 μM Cu(II) immediately returned the Trp fluorescence intensity to that of the native sequence protein. This result is most consistent with a metal binding interaction and seems to rule out that the more efficient quenching observed with QM 212 is the result of conformational differences compared to the native sequence protein.

Competition studies with Cu(II) were performed to examine the interaction of Zn(II) with QM 212. Zinc(II) (100 μM) completely inhibited the Cu(II)-dependent Trp fluorescence quenching (Fig. 3B). This result indicates that at 100 μM Zn(II), the binding site is fully occupied by Zn(II). At 50 μM Zn(II) more Cu(II) quenching was observed (Fig. 3B), and at 10 μM Zn(II) the quenching pattern was similar to that without any added Zn(II). Cadmium(II) also inhibited Cu(II) quenching of the Trp fluorescence, but 500 μM Cd(II) was re-

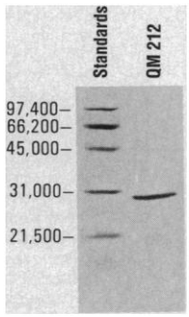

Fig. 2. Twenty percent SDS-PAGE stained with Coomassie blue showing the purified QM 212 and molecular weight standards for comparison. The protein was produced by heat induction for 1 hour at 42°C. The cells were collected and the insoluble material containing the desired protein was isolated by passing the cells twice through a French press followed by centrifugation. The crude protein mixture was solubilized, refolded, and purified according to a modification of the published Genex procedure (*13*). The native sequence protein was also prepared and similarly purified for use in comparative studies. The purified QM 212 and native sequence proteins were dialyzed against EDTA to remove any spurious metals, followed by extensive dialysis in Chelex-treated phosphate buffer.

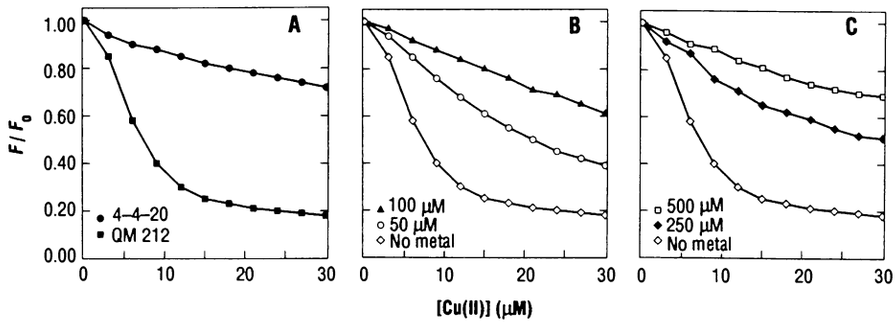

Fig. 3. (**A**) Scaled Trp fluorescence intensities observed for solutions of the native sequence 4-4-20 212 and QM 212 proteins in the presence of 0 to 30 μM $CuCl_2$. The ordinate values correspond to the fluorescence intensity at the given Cu(II) concentration (F) divided by the initial fluorescence intensity observed with no Cu(II) added (F_0). (**B**) Zinc(II) and (**C**) Cd(II) inhibition of Cu(II)-dependent quenching of Trp fluorescence with QM 212; $ZnCl_2$ and $CdCl_2$ were added before addition of $CuCl_2$. Excitation at 292 nm was used for these studies and emission was monitored at 343 nm for QM 212 and 352 nm for the native sequence protein. Conditions: 15 mM sodium phosphate, pH 6.0; 150 nM protein, 1.0-ml total sample volume. Each data point corresponds to the addition of 2 μl of a 1.5 mM aqueous $CuCl_2$ solution, and fluorescence was measured immediately following metal addition and mixing of the sample. All fluorescence measurements were conducted at 23°C in a Shimadzu RF5000V spectrofluorophotometer.

quired to prevent Cu(II)-dependent quenching (Fig. 3C). As opposed to Zn(II), bound Cd(II) displayed a limited ability to quench Trp fluorescence directly. Also, 1.0 mM Mn(II), 1.0 mM Co(II), and 1.0 mM Ni(II) did not inhibit Cu(II) fluorescence quenching, and no direct quenching attributable to binding was observed with these metals, underscoring the selective nature of the QM 212 binding site.

Interestingly, the metal specificity observed with QM 212 is qualitatively similar to that of carbonic anhydrase B. The natural enzyme binds metal in the order Cu(II) > Zn(II) > Cd(II), Ni(II) > Co(II) > Mn(II) (*22*). Despite this similarity in specificity, the binding constants for carbonic anhydrase B are a factor of $\sim 10^6$ greater than those estimated for QM 212. Even so, apparent saturation of the QM 212 metal-binding site with Cu(II) and Zn(II) can be accomplished at metal ion concentrations that should be compatible with catalytic antibody applications. The ability to use both Cu(II) and Zn(II) as cofactors allows consideration of redox as well as hydrolytic reactions.

Upon binding to QM 212, fluorescein fluorescence was quenched in a manner analogous to that of the native sequence protein [Fig. 4A (*13*)]. The residual excitation maxima of bound fluorescein with QM 212 is 508 nm compared with 505 nm for the native sequence protein. A fluorescein binding constant of $3 \times 10^5\ M^{-1}$ was measured for QM 212, which is between three and four orders of magnitude lower than the nonmutant protein. A decrease in binding affinity for fluorescein was expected since two of the modified residues, Ser^{91} and Arg^{34}, make a bifurcated hydrogen bond to fluorescein in the 4-4-20 structure (*14*).

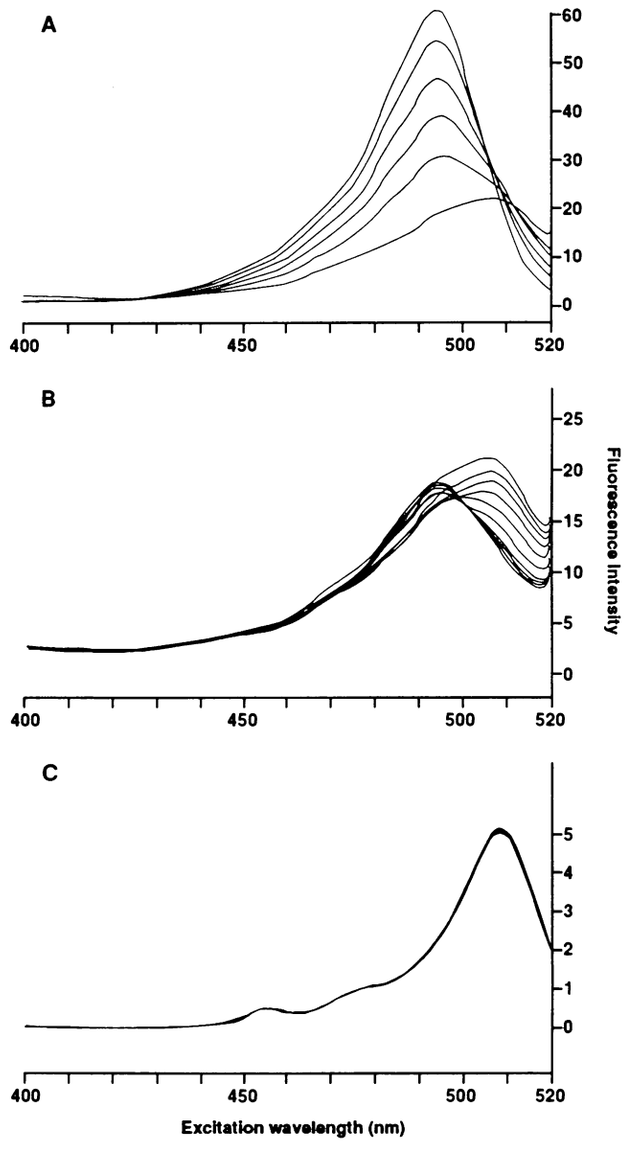

Fig. 4. (**A**) Excitation spectra of fluorescein in the presence of increasing concentrations of QM 212. The uppermost trace corresponds to no QM 212 added and subsequent traces with decreasing fluorescence intensity correspond to QM 212 concentrations of 0.55, 1.1, 2.2, 3.3, and finally 7.7 μM. (**B**) Excitation spectra of fluorescein with 7.7 μM QM 212 in the presence of 0 to 27 μM $CuCl_2$. The uppermost trace corresponds to no $CuCl_2$ added and is identical to the lowermost trace observed in (A). Traces proceeding downward at 508 nm correspond to $CuCl_2$ concentrations of 0 to 27 μM in 3-μM increments. (**C**) Excitation spectra of fluorescein with 800 nM native sequence protein in the presence of 0 to 27 μM $CuCl_2$. In all of these experiments, emission of fluorescein (10.0 nM) was measured at 530 nm with the excitation between 400 nm and 520 nm; total volume was 1.0 ml. Reactions were carried out in 5 mM sodium phosphate (Chelex-treated), pH 8.0. In (B) and (C), 2 μl of 1.5 mM aqueous $CuCl_2$ solution was added sequentially, and the fluorescence was measured immediately after mixing of the sample.

Addition of Cu(II) to a solution containing the native sequence protein with bound fluorescein produced no metal-dependent perturbation of the bound fluorescein fluorescence (Fig. 4C). In contrast, a dramatic effect was again observed with QM 212 protein, as increasing Cu(II) produced a marked decrease in the excitation maxima at 508 nm, leaving a residual peak at 493 nm. Saturation behavior was observed (see Fig. 4B), and since no large increase in the fluorescence intensity at 493 nm was seen (compare A and B in Fig. 4), Cu(II) was apparently not simply displacing fluorescein (*23*). Nevertheless, the precise placement of the metal site must await determination of the x-ray crystal structure of the mutant protein. These results are most consistent with Cu(II) binding simultaneously with fluorescein in the QM 212 binding site. Such simultaneous binding can be viewed as a noncatalytic model for substrate binding to a metalloantibody.

Catalytic metalloantibodies offer an opportunity to combine the enormous potential for substrate recognition of antibodies with the distinctive chemical opportunities afforded by metals. In effect, a particular antibody derived from a combinatorial library might position a catalytically active metal next to a specific locus or face of a substrate. In so doing, the antibody would define the regio or enatio sense of a metal-induced transformation and by using different antibodies, examination or alternative reactive sites on the substrate can be explored.

REFERENCES AND NOTES

1. R. A. Lerner and S. J. Benkovic, *Chemtracts Org. Chem.* **3**, 1 (1990).
2. P. G. Schultz, R. A. Lerner, S. J. Benkovic, *Chem. Eng. News* **68** (no. 22), 26 (1990).
3. L. Sastry *et al.*, *Proc. Natl. Acad. Sci. U.S.A.* **86**, 5728 (1989).
4. E. S. Ward, D. Güssow, A. D. Griffiths, P. T. Jones, G. Winter, *Nature* **341**, 544 (1989); D. Güssow, E. S. Ward, A. D. Griffiths, P. T. Jones, G. Winter, *Cold Spring Harbor Symp. Quant. Biol.* **54**, 265 (1989); R. Orlandi, D. H. Güssow, P. T. Jones, G. Winter, *Proc. Natl. Acad. Sci. U.S.A.* **86**, 3833 (1989).
5. W. D. Huse *et al.*, *Science* **246**, 1275 (1989).
6. S. A. Iverson *et al.*, *Cold Spring Harbor Symp. Quant. Biol.* **54**, 273 (1989).
7. V. A. Roberts *et al.*, *Proc. Natl. Acad. Sci. U.S.A.*, in press.
8. K. K. Kannan *et al.*, *ibid.* **72**, 51 (1975).
9. E. A. Kabat, T. T. Wu, M. Reid-Miller, H. M. Perry, K. S. Gottesman, *Sequences of Proteins of Immunological Interest* (National Institutes of Health, Bethesda, MD, 1987).
10. We examined Cys, Asp, Glu, and His residues within 20 Å of the designed metal binding site to address the possibility of other ligands coordinating the metal (Zn) coincidentally. The nearest possible ligands, Asp^{1}, His^{27D}, and His^{93} [Kabat numbering (*9*)], which have potential binding sites 13 to 16 Å from the Zn atom, could not form bonds to the metal jointly with one of the engineered His residues without major rearrangements in the antibody structure. These rearrangements would involve major changes in the antibody binding site, blocking fluorescein binding, and can therefore be ruled out. In the heavy chain, Glu^{6} and Glu^{46} have their potential Zn binding atoms 13 to 16 Å from the Zn atom. Glu^{6} and Glu^{46} are framework residues separated from the Zn site by β-sheet structure. Only Asp^{101} could be a potential ligand without destroying fluorescein binding. The oxygen atoms of the Asp^{101} side chain are about 4 Å from the Zn atom in our model, so rearrangements would be required.
11. E. D. Getzoff, J. A. Tainer, R. A. Lerner, H. M. Geysen, *Adv. Immunol.* **43**, 1 (1988).
12. C. Chothia *et al.*, *Nature* **342**, 877 (1989).
13. R. E. Bird *et al.*, *Science* **242**, 423 (1988).
14. J. N. Herron, X.-M. He, M. L. Mason, E. W. Voss, Jr., A. B. Edmundson, *Proteins* **5**, 271 (1989).
15. N. I. Nakamaye and F. Eckstein, *Nucleic Acids Res.* **14**, 9679 (1986).
16. D. Scandella, P. Arthur, M. Mattingly, L. Neuhold, *J. Cell Biochem.* **9B**, 203 (1985).
17. M. E. Gottesman, S. Adhya, A. Das, *J. Mol. Biol.* **140**, 57 (1980).
18. R. F. Steiner and E. P. Kirby, *J. Phys. Chem.* **73**, 4130 (1969).
19. J. W. Petrich, J. W. Longworth, G. R. Fleming, *Biochemistry* **26**, 2711 (1987).
20. C. M. Hutnik and A. G. Szabo, *ibid.* **28**, 3935 (1989).
21. J. R. Lakowicz, *Principles of Fluorescence Spectroscopy* (Plenum, New York, 1983).
22. S. Lindskog and P. O. Nyman, *Biochim. Biophys. Acta* **85**, 462 (1964).
23. Alteration of the bound fluorescein excitation spectrum upon addition of Cu(II) is most consistent with a static mechanism implying a metal binding event (*21*, p. 265). Several features of this data in Fig. 4B deserve special comment. First, it is assumed that only properly folded protein can bind fluorescein, so the observed effect of Cu(II) on the bound fluorescein maxima at 508 nm must be occurring in a correctly folded binding pocket. Second, under the conditions chosen for the experiment with QM 212, 70% of the fluorescein was bound and 30% remained in solution, thus explaining the shoulder that remained relatively unchanged at 493 nm. At higher concentrations of Cu(II) and Zn(II) fluorescein was displaced. Third, the perturbed nature of the bound fluorescein excitation maxima indicates that the Cu(II) is bound in close proximity to the fluorescein, offering further evidence that the Cu(II) is binding in the intended three-histidine site.

24. S.A.I. gratefully acknowledges a postdoctoral grant from NIH (F32GM-1204702). V.A.R., E.D.G., and J.A.T. were supported in part by NSF grant DIR-8822385 and NIH grant IGM 37684. We thank the Genex Corporation for their generous gift of the vectors containing the 4-4-20/212 and 4-4-20/202′ genes (*E. coli* strain GX6712), S. Johnson, M. Finkleman, and M. Rollence for advice throughout this project, A. Edmundson for the use of x-ray coordinates that are pending deposition in the Brookhaven Protein Data Bank, and S. Danishefsky, D. Millar, and W. Wade for many enlightening discussions relating to this work. We commend R. T. Samodal for essential and superior technical assistance with protein purification.

14 May 1990; accepted 25 June 1990

A G Protein Mutant That Inhibits Thrombin and Purinergic Receptor Activation of Phospholipase A_2

SUNIL K. GUPTA, EMILIO DIEZ, LYNN E. HEASLEY, SHOJI OSAWA, GARY L. JOHNSON

The stimulation of phospholipase A_2 by thrombin and type 2 (P_2)–purinergic receptor agonists in Chinese hamster ovary cells is mediated by the G protein G_i. To delineate α chain regulatory regions responsible for control of phospholipase A_2, chimeric cDNAs were constructed in which different lengths of the α subunit of G_s (α_s) were replaced with the corresponding sequence of the G_i α subunit (α_{i2}). When a carboxyl-terminal chimera $\alpha_{s\text{-}i(38)}$, which has the last 38 amino acids of α_s substituted with the last 36 residues of α_{i2}, was expressed in Chinese hamster ovary cells, the receptor-stimulated phospholipase A_2 activity was inhibited, although the chimera could still activate adenylyl cyclase. Thus, $\alpha_{s\text{-}i(38)}$ is an active α_s, but also a dominant negative α_i molecule, indicating that the last 36 amino acids of α_{i2} are a critical domain for G protein regulation of phospholipase A_2 activity.

THE RELATED G PROTEINS G_s AND G_i stimulate and inhibit adenylyl cyclase, respectively. The α_s and α_i subunit polypeptides are ~65% homologous in primary sequence (*1–3*) and share common βγ subunits (*4*), but selectively couple to different receptors (*5*). Despite their initial identification as inhibitors of adenylyl cyclase, the primary function of G_i proteins may actually be the regulation of ion channels, phospholipase A_2, and possibly phospholipase C (*6–8*). It has been concluded that G_i-like proteins regulate receptor-coupled phospholipases because these pathways are inhibited by treatment of cells with pertussis toxin, which adenosine diphosphate (ADP) ribosylates and inhibits G_i and G_o proteins (*9–11*), and because guanosine triphosphate (GTP) analogs stimulate phospholipase activities in permeabilized cells and membranes (*7, 8*).

S. K. Gupta, L. E. Heasley, S. Osawa, G. L. Johnson, Division of Basic Sciences, National Jewish Center for Immunology and Respiratory Medicine, Denver, CO 80206, and Department of Pharmacology, University of Colorado Medical School, Denver, CO 80262.
E. Diez, Smith, Kline and Beecham Pharmaceuticals, Department of Immunology, King of Prussia, PA 19406–0930.